

RISE based Synchronous Control of Dual Electro-hydraulic Servo System via Internal Force Adjustment

Yinghao Yang, Zhenle Dong, Zhigang Zhou, Zheng Zhang, Geqiang Li, Yugong Dang

Abstract—For the issue of synchronous driving of dual electro-hydraulic servo system, a novel synchronous control method via internal force adjustment based on robust integral of the sign of the error (RISE) is proposed. The nonlinear mathematical model of electro-hydraulic servo system considering unmodeled disturbance is established. The synchronous motion error of dual electro-hydraulic servo system is regarded as the cause of the internal force. In order to eliminate synchronous motion error, the internal force adjustment controller is designed based on the RISE method and further it is integrated with the original PID controller of the system. Based on Lyapunov analysis, it is proved that the internal force can be asymptotically adjusted to zero theoretically. Comparative tracking verification under two position command working conditions is carried out and the simulation results show that the proposed control strategy can improve the synchronous accuracy.

Index Terms—electro-hydraulic servo system, internal force, robust integral of the sign of the error, synchronous control

I. INTRODUCTION

MULTIPLE hydraulic synchronous actuators are widely used in equipment manufacturing, aviation, construction machinery and other fields[1-3], and their performance depends on the execution accuracy of single actuator and the synchronous accuracy of multiple actuators. When multiple hydraulic actuators driving the same load, regardless of the hydraulic actuators are in the same direction or in the opposite direction, due to the influence of the manufacturing accuracy and unknown environmental disturbance, the level of

wear and leakage of various components will be different after the system runs for a certain period of time. At this time, the control accuracy of each actuator will be different, and the synchronous error of multiple actuators will increase, which will seriously restrict the system performance[4]. Therefore, it is necessary to develop excellent synchronous control algorithm to improve the performance and eliminate the motion difference of multiple hydraulic actuators through software methods and make up for the non-synchronization caused by hardware facilities. In this regard, many researchers have done a lot of research on the hydraulic synchronous control algorithm.

Classical PID control does not need to consider model factors. Although widely applied, it has limited control accuracy for nonlinear systems and is prone to overshoot and oscillation. Chen[5] proposed a fuzzy PID controller and the controller parameters are adjusted online through fuzzy rules to improve the system synchronous accuracy. Wu[6] proposed a fuzzy single neuron PID control algorithm for the hydraulic synchronous control of double cylinders in a forging machine, which has stronger robustness than the traditional fuzzy PID control. The control method based on RBF neural network sliding mode control proposed by Li[7] shows high tracking accuracy and fast response to the given signal. Yao[8] proposed a state feedback fuzzy controller based on random input-delay, which has stronger robustness than the traditional fuzzy controller. Felipe [9] proposed a robust multivariable adaptive control technique for time varying autoregressive moving average systems with exogenous inputs considering identification and auto-tuning.

A valuable synchronous perspective was presented by Wen[10] that "Force control dose not affect object motion, although object motion does affect the internal force ", which gives us inspiration that internal force adjustment can be a new idea for electro-hydraulic servo synchronous control.

Recently, Xian [11] proposed RISE (robust integral of the sign of the error) controller to deal with the uncertainties of a class of high-order, multi-input and multi-output nonlinear systems. It has the advantage of achieving asymptotic stability without using high-gain feedback [12] and has been applied in the fields of friction recognition, vision system range prediction and error detection and recognition.[13-15]

On the basis of the above analysis, we consider synchronous control as the control of the internal force between the actuators. The nonlinear mathematical model of electro-hydraulic servo system considering unmodeled disturbance is established, and a synchronous control strategy via

Manuscript received January 23, 2022; revised July 27, 2022. This work was supported in part by Natural Science Foundation of Henan Province of China under Grant 202300410142, in part by Open Foundation of the State Key Laboratory of Fluid Power and Mechatronics Systems under Grant GZKF-202117, in part by Key Research and Development and Promotion Special Project of Henan Province under Grant GZKF-202117.

Yinghao Yang is a Postgraduate student of the School of Vehicle Engineering, Henan University of Science and Technology. Luoyang 471000, China (e-mail: yangyinghao06@163.com).

Zhenle Dong is a Lecturer of the School of Vehicle Engineering, Henan University of Science and Technology. Luoyang 471000, China (Corresponding author, e-mail: dong_zhenle@163.com).

Zhigang Zhou is an Associate Professor of the School of Vehicle Engineering, Henan University of Science and Technology. Luoyang 471000, China (e-mail: hnmcczzg@163.com)

Zheng Zhang is a Postgraduate student of the School of Vehicle Engineering, Henan University of Science and Technology. Luoyang 471000, China (e-mail: zhangzheng987789@163.com).

Geqiang Li is a Professor in the Collaborative Innovation Center of Machinery Equipment Advanced Manufacturing of Henan Province, Luoyang 4710003, Henan, China (e-mail: hitligeqiang@163.com).

Yugong Dang is an Associate Professor of the School of Vehicle Engineering, Henan University of Science and Technology. Luoyang 471000, China (e-mail: dang_2000@163.com)

internal force adjustment based on RISE method is proposed.

The paper is organized as follows: The nonlinear mathematical model is established in Section II, the complete controller design process and control performance description are presented in Section III, the comparative simulation setup and result analysis are presented in Section IV, and the last part gives the conclusion and future research.

II. MATHEMATICAL MODELING

The working principle of the considered valve-controlled electro-hydraulic servo synchronous control system is shown in Figure 1. Both subsystems act on the same inertial load through the servo valve-controlled single-rod hydraulic cylinder.

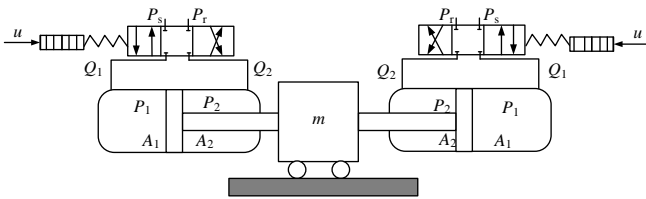


Fig. 1. Structure diagram of dual electro-hydraulic servo control system

The kinematic equation of the electro-hydraulic servo system is:

$$m\ddot{y} = P_1 A_1 - P_2 A_2 - B\dot{y} - A_f S_f(\dot{y}) - f(y, \dot{y}, t) \quad (1)$$

where m , y , \dot{y} , \ddot{y} represent the load mass, displacement, velocity and acceleration respectively, A_1 , A_2 represent the effective piston area of the left and right chambers of hydraulic cylinder, P_1 , P_2 represent the oil pressure of the two chambers of hydraulic cylinder respectively, B is the effective viscous damping coefficient, A_f , S_f represent the amplitude and the continuously approximate shape function that can be modeled of coulomb friction respectively, $f(y, \dot{y}, t)$ is the unmodeled dynamics.

The pressure dynamic of the two-chamber is:

$$\dot{P}_1 = \frac{\beta_e}{V_1} (-A_1 \dot{y} - C_l P_L + Q_1) \quad (2)$$

$$\dot{P}_2 = \frac{\beta_e}{V_2} (A_2 \dot{y} + C_l P_L - Q_2) \quad (3)$$

where β_e is the elasticity modulus of the hydraulic oil, $V_1 = V_{01} + A_1 y$, $V_2 = V_{02} - A_2 y$ represent the control volume of the left and right chambers of hydraulic cylinder respectively, V_{01} and V_{02} represent the initial control volume of the left and right chambers, Q_1 , Q_2 denote the into/out hydraulic flow of the left/right cavity of the hydraulic cylinder respectively, C_l is the internal leakage factor, $P_L = P_1 - P_2$ is the load pressure.

The load flow equation of servo valve is:

$$Q_1 = \sqrt{2} k_{q1} x_v \left[s(x_v) \sqrt{(P_s - P_1)} + s(-x_v) \sqrt{(P_1 - P_r)} \right] \quad (4)$$

$$Q_2 = \sqrt{2} k_{q2} x_v \left[s(x_v) \sqrt{(P_2 - P_r)} + s(-x_v) \sqrt{(P_s - P_2)} \right] \quad (5)$$

$$k_{q1} = C_d w_1 \sqrt{\frac{1}{\rho}}, k_{q2} = C_d w_2 \sqrt{\frac{1}{\rho}} \quad (6)$$

and $s(*)$ is defined as:

$$s(*) = \begin{cases} 1, & \text{if } * \geq 0 \\ 0, & \text{if } * < 0 \end{cases} \quad (7)$$

where k_{q1} , k_{q2} denote the flow gain at the left and right ends of the spool displacement of the servo valve respectively, x_v , P_s , P_r , C_d , ρ represent spool displacement, supply pressure, return pressure, orifice flow coefficient of servo valve, hydraulic oil density respectively, w_1 , w_2 represent the area gradient at the left and right ends of the orifice of servo valve spool respectively.

Assumption 1: Servo valve is symmetrical and matched, i.e., $k_{q1} = k_{q2} = k_q$. The elasticity modulus of the hydraulic oil in the two cavities of the actuator is the same, i.e., $\beta_{e1} = \beta_{e2} = \beta_e$. The frequency bandwidth of the servo valve is much higher than that of the system, which can simplify the dynamics of the servo valve as a proportional term, i.e. $x_v = k_i u$, so $s(x_v) = s(u)$. The system works under normal working conditions, that is, the pressure in the two actuator chambers meets $0 < P_r < P_1 < P_s$, $0 < P_r < P_2 < P_s$.

Based on the above assumptions, equations (4) and (5) can be transformed to

$$Q_1 = g R_1 u \quad (8)$$

$$Q_2 = g R_2 u \quad (9)$$

where $g = \sqrt{2} k_q k_i$, and

$$R_1 = \left[s(u) \sqrt{P_s - P_1} + s(-u) \sqrt{P_1 - P_r} \right] \quad (10)$$

$$R_2 = \left[s(u) \sqrt{P_2 - P_r} + s(-u) \sqrt{P_s - P_2} \right] \quad (11)$$

Therefore, equations (1-3) and (8-11) characterize the nonlinear model of the electro-hydraulic servo system., and subsequent controller design will be derived based on this nonlinear model.

III. INTERNAL FORCE CONTROLLER DESIGN

When the motion of the dual electro-hydraulic servo control system is not synchronized, synchronous error will cause the driving interference between the two hydraulic cylinders, thereby generating internal force. The goal of controller design is to eliminate the internal force.

Define $F = m\ddot{y}$, then from equation (1)(2)(3), we can get

$$\begin{aligned} \dot{F} = & \left(\frac{A_1}{V_1} R_1 + \frac{A_2}{V_2} R_2 \right) g \beta_e u - \left(\frac{A_1^2}{V_1} + \frac{A_2^2}{V_2} \right) \beta_e \dot{y} \\ & - \left(\frac{A_1}{V_1} + \frac{A_2}{V_2} \right) \beta_e C_l P_L - B\ddot{y} - A_f \dot{S}_f - \dot{f} \end{aligned} \quad (12)$$

Considering the parametric uncertainties, it is difficult to obtain accurate values of system parameters β_e , C_l , B , A_f , so nominal values are used in controller design, and the model uncertainties caused by parametric deviations between accurate values and nominal values can be seen as disturbances.

Define β_{en} , C_{ln} , B_n , A_{fn} as the nominal value of β_e , C_l , B , A_f respectively, then equation (12) can be transformed to

$$\begin{aligned} \dot{F} = & \left(\frac{A_1}{V_1} R_1 + \frac{A_2}{V_2} R_2 \right) g \beta_{en} u - \left(\frac{A_1^2}{V_1} + \frac{A_2^2}{V_2} \right) \beta_{en} \dot{y} \\ & - \left(\frac{A_1}{V_1} + \frac{A_2}{V_2} \right) \beta_{en} C_{ln} P_L - B_n \ddot{y} - A_{fn} \dot{S}_f + \Delta \\ = & g_3 u - f_c - f_u - B_n \ddot{y} - A_{fn} \dot{S}_f + \Delta \end{aligned} \quad (13)$$

where

$$\begin{aligned} \Delta &= -\left(\frac{A_1 R_1}{V_1} + \frac{A_2 R_2}{V_2}\right) g(\beta_{en} - \beta_e) u + \left(\frac{A_1^2}{V_1} + \frac{A_2^2}{V_2}\right) (\beta_{en} - \beta_e) \dot{y} \\ &+ \left(\frac{A_1}{V_1} + \frac{A_2}{V_2}\right) (\beta_{en} C_{in} - \beta_e C_t) P_L - (B_n - B) \ddot{y} - (A_{in} - A_f) \dot{S}_f - \dot{f} \\ g_3 &= \left(\frac{A_1}{V_1} R_1 + \frac{A_2}{V_2} R_2\right) g \beta_{en}, \quad f_c = \left(\frac{A_1^2}{V_1} + \frac{A_2^2}{V_2}\right) \beta_{en} C_{in} \\ f_u &= \left(\frac{A_1}{V_1} + \frac{A_2}{V_2}\right) \beta_{en} C_{in} P_L \end{aligned}$$

From the expressions of R_1, R_2 and V_1, V_2 , it can be known that following inequality is always true:

$$g_3 > 0$$

Assumption 2: The lumped system uncertainties Δ is third-order continuous differentiable and bounded, i.e.,

$$|\Delta|, |\dot{\Delta}|, |\ddot{\Delta}| \in L_\infty$$

and

$$|\dot{\Delta}| \leq \xi_{N_2}, |\ddot{\Delta}| \leq \xi_{N_3}$$

and the bounds ξ_{N_2}, ξ_{N_3} are known.

Define the following error variables:

$$e_f = F - F_d, \quad r = \dot{e}_f + k_1 e_f \quad (14)$$

where k_1 is a positive feedback gain, F_d is the desired internal force. To eliminate the internal force, the desired internal force should be chosen as zero.

From equation (13)(14), we have

$$\begin{aligned} r &= \dot{e}_f + k_1 e_f \\ &= g_3 u - f_c - f_u - B_n \ddot{y} - A_{in} \dot{S}_f + \Delta - F_{eq} \\ F_{eq} &= \dot{F}_d - k_1 e_f \end{aligned} \quad (15)$$

Finally, the controller is designed as follows:

$$\begin{aligned} u &= u_{F1} + u_{F2} + u_{F3} \\ u_{F1} &= \frac{1}{g_3} (f_c + f_u + B_n \ddot{y} + A_{in} \dot{S}_f + F_{eq}) \\ u_{F2} &= -k_2 e_f \\ u_{F3} &= -\int_0^t k_r k_1 e_f + K \text{sign}(e_f) du \end{aligned} \quad (16)$$

where $k_r > 0, k_2 > 0$ is the controller gain to be chosen, $K > 0$ is the robust gain, u_{F1}, u_{F2}, u_{F3} represent the model compensation term, linear robust stability term, and nonlinear robust integral of the sign of the error (RISE) respectively. Especially, u_{F3} is mainly used to deal with the lumped uncertainties Δ to improve the internal force control accuracy. It should be noted that in the actual application of the proposed controller, there is no need to calculate the auxiliary error signal r .

IV. MAIN RESULTS

Substituting the final control (16) into equation (15), we can achieve

$$r = -k_r e_f - \int_0^t k_r k_1 e_f + K \text{sign}(e_f) + \Delta \quad (17)$$

Take the time derivative of (17), we have :

$$\dot{r} = \dot{\Delta} - k_r r - K \text{sign}(e_f) \quad (18)$$

In order to facilitate the performance analysis of the controller, the following lemma is given.

Lemma 1: Define auxiliary function $L(t), P(t)$ as follows^[11]:

$$L(t) = r \left[\dot{\Delta} - K \text{sign}(e_f) \right] \quad (19)$$

$$P(t) = K |e_f(0)| - e_f(0) \dot{\Delta}(0) - \int_0^t L(\tau) d\tau$$

If the robust gain K satisfies the following inequality:

$$K > \xi_{N_2} + \frac{1}{k_1} \xi_{N_3} \quad (20)$$

then the auxiliary function $P(t)$ is always positive.

Proof of Lemma 1:

Substitute (14) into (19) and then integrating in time, we can obtain

$$\begin{aligned} \int_0^t L(t) dt &= \int_0^t k_1 e_f(t) (\dot{\Delta}(t) - K \text{sign}(e_f(t))) dt \\ &+ \int_0^t \frac{d(e_f(t))}{dt} \dot{\Delta}(t) dt - \int_0^t K \frac{d(e_f(t))}{dt} \text{sign}(e_f(t)) dt \end{aligned} \quad (21)$$

We now upper bound the right-hand side of (21) as

$$\begin{aligned} \int_0^t L(t) dt &= \int_0^t k_1 e_f(t) (\dot{\Delta}(t) - K \text{sign}(e_f(t))) dt + e_f(t) \dot{\Delta}(t) \Big|_0^t \\ &- \int_0^t e_f(t) \frac{d\dot{\Delta}(t)}{dt} dt - K |e_f(t)| \Big|_0^t \\ &= \int_0^t k_1 e_f(t) \times \left(\dot{\Delta}(t) - \frac{1}{k_1} \frac{d\dot{\Delta}(t)}{dt} K \text{sign}(e_f(t)) \right) dt \\ &+ e_f(t) \dot{\Delta}(t) - e_f(0) \dot{\Delta}(0) - K |e_f(t)| + K |e_f(0)| \end{aligned} \quad (22)$$

After the partial integration of the right-hand side of (22), we have

$$\begin{aligned} \int_0^t L(t) dt &\leq \int_0^t k_1 |e_f(t)| \left(|\dot{\Delta}(t)| + \frac{1}{k_1} \left| \frac{d\dot{\Delta}(t)}{dt} \right| - K \right) dt \\ &+ |e_f(t)| (|\dot{\Delta}(t)| - K) + K |e_f(0)| - e_f(0) \dot{\Delta}(0) \end{aligned} \quad (23)$$

Form (23) and Assumption 2, it is easy to see that if K is chosen according to (20), then the auxiliary function $P(t)$ is always positive. The proof of Lemma 1 is completed.

Theorem 1: For system (13), if the robust gain K in controller (16) satisfies the inequality (20), and the value of the feedback gain k_2, k_r are large enough so that the matrix Λ defined as follows is a positive definite matrix:

$$\Lambda = \begin{bmatrix} k_1 & -\frac{1}{2} \\ -\frac{1}{2} & k_r \end{bmatrix} \quad (24)$$

then all signals in the closed-loop system are bounded, and the robust controller can obtain asymptotic tracking performance. That is, $e_f \rightarrow 0$ as $t \rightarrow \infty$.

Proof of Theorem 1:

Define the following Lyapunov function:

$$V = \frac{1}{2} e_f^2 + \frac{1}{2} r^2 + P \quad (25)$$

Take the time derivative of V , and substitute (14)(18), we have

$$\begin{aligned} \dot{V} &= e_f \dot{e}_f + r \dot{r} + \dot{P} \\ &= e_f (r - k_1 e_f) + r \left[\dot{\Delta} - k_r r - K \text{sgn}(e_f) \right] \\ &- r N + r K \text{sgn}(e_f) \\ &\leq -\lambda_{\min}(\Lambda) (e_f^2 + r^2) = -W \end{aligned} \quad (26)$$

From (26), it can be seen that V is bounded, so e_f , r are bounded, and then from (16) we know all the signals of the closed-loop system are bounded, so $\dot{W} \in L_\infty$. Then from (14)(18), it is easy to check that $W \in L_2$. So W is uniformly continuous. Based on the Barbalet's Lemma[16-17], $W \rightarrow 0$ as $t \rightarrow \infty$, i.e., $e_f \rightarrow 0$. Then complete the proof.

The synchronous control principle of the proposed RISE-based internal force adjustment is shown in Figure 2.

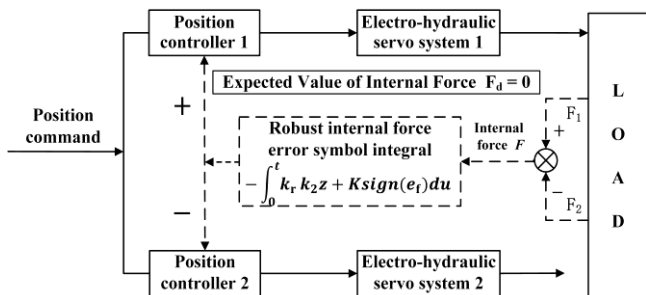


Fig. 2. Schematic diagram of internal force adjustment synchronous control based on RISE method

V. SIMULATION COMPARISON

The parameter of the considered electro-hydraulic servo system is shown in Table 1. To simulate the different levels of the component wear and leakage of the two subsystems, the effective viscous damping coefficient, hydraulic oil elasticity modulus, and leakage coefficient of the two subsystems in the table are taken different values.

TABLE I
PARAMETERS OF THE CONTROL SYSTEM

Symbol	Unit	Value
m	kg	40
A_1, A_2	m^2	$2e-4$
V_{01}, V_{02}	m^3	$1e-3$
A_f	N	10
P_s	Pa	$7e6$
P_r	Pa	0
g	$m^4 * (s * V * \sqrt{N})^{-1}$	$4e-8 / \sqrt{2}$
B_1, B_2	$N * s / m$	80, 140
β_{e1}, β_{e2}	Pa	$20e7, 15e7$
C_{t1}, C_{t2}	$m^5 / (N * s)$	$9e-12, 40e-12$

Assume that the original position controller of the system is a PID controller, the asynchronous operation of two hydraulic cylinders can be simulated through the parameter settings in Table 1. The simulation platform is built based on the MATLAB/Simulink. In order to verify the effectiveness of the proposed controller, the following three controllers were selected for comparison.

(1) C1: This is the PID controller and the controllers parameters are selected as : $k_p=10, k_i=120, k_d=0$ which denotes the P-gain, I-gain, D-gain respectively.

(2) The proposed controller, i.e., PID with RISE-based internal force adjustment: the controller parameters are chosen as $k_p=10, k_i=120, k_d=0$ and $k_r=3e-5, k_1=10e-4, K=0.05$.

(3) C2: This is PID with proportional internal force ad-

justment. Compared with the proposed controller, this controller only integrates the proportional internal force adjustment, that is, u_{F2} in equation (16), on the basis of PID. The corresponding controller parameters are chosen the same as the proposed controller.

Remark 1: In the verification, on the basis of the original PID controller, we integrated the designed RISE-based internal force adjustment. However, to avoid repetitive model compensation, only the linear stability term u_{F2} and the robust integral of sign of the error u_{F3} are integrated.

Case 1: Sine signal tracking case.

The position command is chosen as $y = \sin(t) m$ shown in Figure 3. The simulation step is set as 0.005s and the simulation time is taken as 50s.

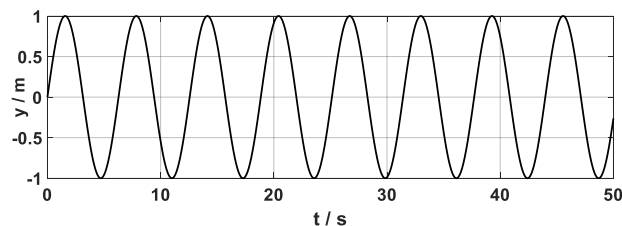


Fig. 3. The desired position trajectory in case 1

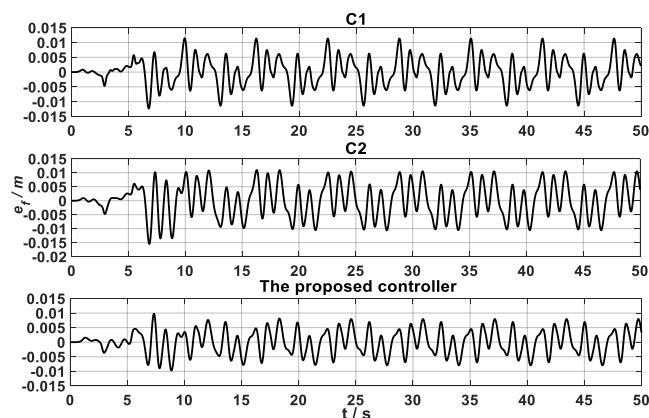


Fig. 4. Tracking errors of the compared controllers

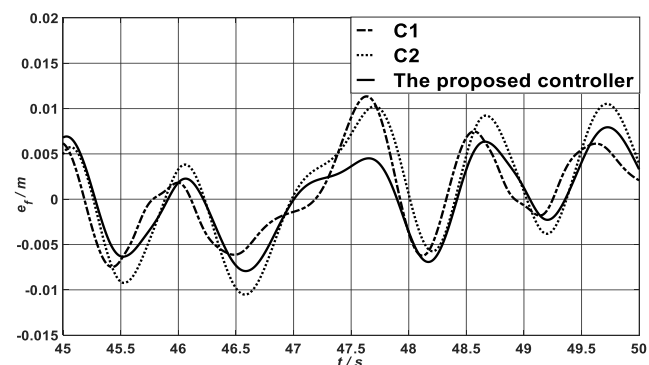


Fig. 5. Tracking errors for 45-50s

TABLE II
THE MAXIMUM SYNCHRONIZATION ERROR OF THE THREE CONTROLLERS AT DIFFERENT TIME PERIODS

PERIOD	C1/m	C2/m	The proposed controller/m
0-10s	$1.14e-02$	$1.02e-02$	$9.76e-03$
10-30s	$1.13e-02$	$1.09e-02$	$8.12e-03$
30-50s	$1.13e-02$	$1.05e-02$	$7.93e-03$

It can be seen from Figure 4 that the maximum synchronous error of C1 controller is $1.14e-02m$, the maximum synchronous error of C2 controller is $1.09e-02m$, while the maximum synchronization error of the proposed controller is $9.76e-03m$. It can be seen from Figure 5 and Table 2 that the maximum synchronous error of C2 controller is reduced by about 15% compared with C1 controller, and the maximum synchronous error of the proposed controller is further reduced by 20%. Then we know that for sine tracking case, the proposed controller performs better than the other two controllers in eliminating the influence of uncertainty disturbance.

Case 2: Square wave signal tracking case

The amplitude of the square wave signal is 0.1m as shown in Figure 6. The simulation step is 0.005s, and the simulation time is 50s.

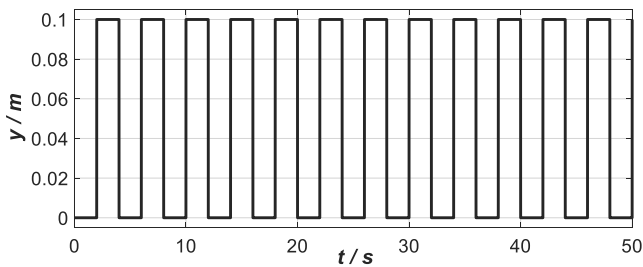


Fig. 6. The desired position trajectory in case 2

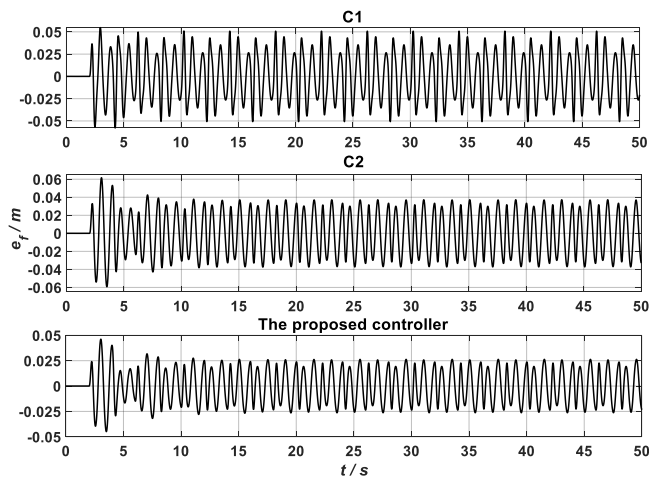


Fig. 7. Tracking errors of the compared controllers

It can be seen from Figure 7 that the maximum synchronous error of C1 controller is $5.09e-02m$, the maximum synchronous error of C2 controller is $6.16e-02m$, while the maximum synchronous error of the proposed controller is $4.62e-03m$.

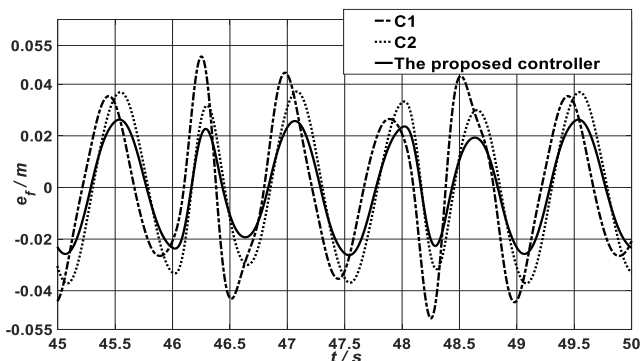


Fig.8. Tracking errors for 45-50s

TABLE III
THE MAXIMUM SYNCHRONIZATION ERROR OF THE THREE CONTROLLERS AT DIFFERENT TIME PERIODS

PERIOD	C1/m	C2/m	The proposed controller/m
0-10s	5.47e-02	6.16e-02	4.61e-02
10-30s	5.09e-02	3.79e-02	2.75e-02
30-50s	5.07e-02	3.71e-02	2.63e-02

From Figure 8 and Table 3, it can be seen that the maximum synchronous error of C2 controller is reduced by about 20% compared with C1 controller, and the maximum synchronous error of the proposed controller is further reduced by 25% compared with compared with C2 controller. Then we know that under the square wave tracking case, the proposed controller performs better than the other two controllers in eliminating the influence of uncertainty disturbance.

VI. CONCLUSION

For the synchronous driving problem of dual electro-hydraulic servo systems, a RISE-based internal force adjustment synchronous control method is proposed to eliminate the internal force. Through simulation and comparison analysis, it is verified that the designed controller can reduce the maximum synchronous error by more than 20% compared with the original PID controller and PID with internal force proportional adjustment controller, and can eventually improve the synchronous accuracy significantly. Future research will focus on the tracking control at higher frequency commands and how to compensate the nonlinear friction at ultra-low speeds.

REFERENCES

- [1] Z. Zuo, W. Shen, Z. Huang, X. Huang, "Development of dual hydraulic cylinder synchronous control system based on LabVIEW," *Machine Tools and Hydraulics*, vol. 43, no. 02, pp. 83-85, 2015.
- [2] C. Chen, "Research on multi cylinder synchronous control technology of hydraulic system," *Mechanical and Electronic*, vol. 34, no. 07, pp. 42-45, 2016.
- [3] S. Cheng, Q. Zhang, "A new type of module docking device for large structures and multi cylinder synchronous control," *China Mechanical Engineering*, vol. 29, no. 10, pp. 1214-1219+1226, 2018.
- [4] Y. Ye, J. Hu, X. Zhang, B. Chen, "Analysis and application of hydraulic synchronization system," *Mechanical Engineering and Automation*, no. 03, pp. 172-174+177, 2021.
- [5] L. Chen, Z. Hong, "Design of fuzzy PID controller for electro-hydraulic servo system," *Electronic Test*, no. 11, pp. 51-52+48, 2021.
- [6] N. Wu, M. Yuan, "Modeling and Simulation of two cylinder hydraulic synchronous control system of forging machine," *Forging Technology*, vol. 45, no. 01, pp. 144-150, 2020.
- [7] W. Li, G. Shi, "RBF neural network sliding mode control of electro-hydraulic servo system," *Hydraulic and Pneumatic*, no. 02, pp. 109-114, 2019.
- [8] H. Yao, "Augmented Lyapunov Function-based Exponential Stability Control of Fuzzy Systems with Stochastic Input Delay," *IAENG International Journal of Applied Mathematics*, vol. 51, no. 1, pp. 41-47, 2021.
- [9] F. Osorio-Arteaga, J. J. Marulanda-Durango, E. Giraldo, "Robust Multivariable Adaptive Control of Time-varying Systems," *IAENG International Journal of Computer Science*, vol. 47, no. 4, pp. 605-612, 2020.
- [10] J. Wen, K. Kreutz-Delgado, "Motion and force control of multiple robotic manipulators," *Automatica*, vol. 28, no. 4, pp. 729-743, 1992.
- [11] B. Xian, D. M. Dawson, M. S. de Queiroz, J. Chen, "A continuous asymptotic tracking control strategy for uncertain nonlinear systems," *IEEE Transactions on Automatic Control*, vol. 49, no. 7, pp. 1206-1211, 2004.

- [12] B. Xian, M. S. De Queiroz, D. M. Dawson, M. L. McIntyre, "A discontinuous output feedback controller and velocity observer for nonlinear mechanical systems," *Automatica*, vol. 40, no. 4, pp. 695-700, 2004.
- [13] C. Makkar, G. Hu, W. G. Sawyer, W. E. Dixon, "Lyapunov-based tracking control in the presence of uncertain nonlinear parameterizable friction," *IEEE Transactions on Automatic Control*, vol. 52, no. 10, pp. 1988-1994, 2007.
- [14] M. L. McIntyre, W. E. Dixon, D. M. Dawson, I. D. Walker, "Fault identification for robot manipulators," *IEEE Transactions on Robotics*, vol. 21, no. 5, pp. 1028-1034, 2005.
- [15] W. E. Dixon, Y. Fang, D. M. Dawson, T. J. Flynn, "Range Identification for Perspective Vision Systems," *IEEE Transactions on Automatic Control*, vol. 48, no. 12, pp. 2232-2238, 2003.
- [16] K. S. Narendra, A. M. Annaswamy, "A new adaptive law for robust adaptation without persistent excitation," *IEEE Transactions on Automatic Control*, vol. AC-32, no. 2, pp. 134-145, 1987.
- [17] Y.-Q. Zhou, X.-Y. Ouyang, N.-N. Zhao, H.-B. Xu, H. Li, "Prescribed Performance Adaptive Neural Network Tracking Control of Strict-Feedback Nonlinear Systems with Nonsymmetric Dead-zone," *IAENG International Journal of Applied Mathematics*, vol. 51, no. 3, pp. 444-452, 2021.